

Constrained Minimal Supersymmetric Standard Model with Generalized Yukawa Quasi-Unification

N. Karagiannakis,^{1,*} G. Lazarides,^{1,†} and C. Pallis^{2,‡}

¹*Physics Division, School of Technology, Aristotle University of Thessaloniki, Thessaloniki 54124, Greece*

²*Department of Physics, University of Cyprus, P.O. Box 20537, CY-1678 Nicosia, CYPRUS*

(Dated: September 10, 2018)

We analyze the constrained minimal supersymmetric standard model with $\mu > 0$ supplemented by a generalized ‘asymptotic’ Yukawa coupling quasi-unification condition, which allows an acceptable b -quark mass. We impose constraints from the cold dark matter abundance in the universe, B physics, and the mass m_h of the lightest neutral CP-even Higgs boson. We find that, in contrast to previous results with a more restrictive Yukawa quasi-unification condition, the lightest neutralino $\tilde{\chi}$ can act as a cold dark matter candidate in a relatively wide parameter range. In this range, the lightest neutralino relic abundance is drastically reduced mainly by stau-antistau coannihilations and, thus, the upper bound on this abundance from cold dark matter considerations becomes compatible with the recent data on the branching ratio of $B_s \rightarrow \mu^+ \mu^-$. Also, $m_h \simeq (125 - 126)$ GeV, favored by LHC, can be easily accommodated. The mass of $\tilde{\chi}$, though, comes out large (~ 1 TeV).

PACS numbers: 12.10.Kt, 12.60.Jv, 95.35.+d

I. INTRODUCTION

The recently announced experimental data on the mass of the *standard model* (SM)-like Higgs boson [1–3] as well as the branching ratio $\text{BR}(B_s \rightarrow \mu^+ \mu^-)$ of the process $B_s \rightarrow \mu^+ \mu^-$ [4] in conjunction with *cold dark matter* (CDM) considerations [5] put under considerable stress [6] the parameter space of the *constrained minimal supersymmetric standard model* (CMSSM) [7–10]. Let us recall that the CMSSM is a highly predictive version of the *minimal supersymmetric standard model* (MSSM) based on universal boundary conditions for the soft supersymmetry (SUSY) breaking parameters. The free parameters of the CMSSM are

$$\text{sign}\mu, \tan\beta, M_{1/2}, m_0, \text{ and } A_0, \quad (1)$$

where $\text{sign}\mu$ is the sign of μ , the mass parameter mixing the electroweak Higgs superfields H_2 and H_1 of the MSSM which couple to the up- and down-type quarks respectively, $\tan\beta$ is the ratio of the *vacuum expectation values* (VEVs) of H_2 and H_1 , and the remaining symbols above denote the common gaugino mass, the common scalar mass, and the common trilinear scalar coupling constant, respectively, defined at the *grand unified theory* (GUT) scale M_{GUT} determined by the unification of the gauge coupling constants.

It would be interesting to investigate the consequences of these experimental findings for even more restricted versions of the CMSSM which can emerge by embedding it in a SUSY GUT model with a gauge group containing $SU(4)_c$ and $SU(2)_R$. This can lead [11] to ‘asymptotic’

Yukawa unification (YU) [12], i.e. the exact unification of the third generation Yukawa coupling constants (of the top [bottom] quark h_t [h_b] and the tau lepton h_τ) at M_{GUT} . The conditions for this to hold are that the electroweak Higgs superfields H_2 , H_1 as well as the third generation right handed quark superfields form $SU(2)_R$ doublets, the third generation quark and lepton $SU(2)_L$ doublets [singlets] form a $SU(4)_c$ 4-plet [$\bar{4}$ -plet], and the Higgs doublet H_1 which couples to them is a $SU(4)_c$ singlet. The simplest GUT gauge group which contains both $SU(4)_c$ and $SU(2)_R$ is the *Pati-Salam* (PS) group $G_{\text{PS}} = SU(4)_c \times SU(2)_L \times SU(2)_R$ [13, 14].

It is well-known that, given the experimental values of the top-quark and tau-lepton masses (which, combined with YU, naturally restrict $\tan\beta$ to large values), the CMSSM supplemented by the assumption of YU yields unacceptable values of the b -quark mass m_b for both signs of μ . This is due to the generation of sizable SUSY corrections [15] to m_b (about 20%), which arise from sbottom-gluino (mainly) and stop-chargino loops [15, 16] and have the same sign as μ – with the standard sign convention of Ref. [17]. The predicted tree-level $m_b(M_Z)$, which turns out to be close to the upper edge of its 95% *confidence level* (c.l.) experimental range, receives, for $\mu > 0$ [$\mu < 0$], large positive [negative] corrections which drive it well above [a little below] the allowed range. Consequently, for both signs of μ , YU leads to an unacceptable $m_b(M_Z)$ with the $\mu < 0$ case being much less disfavored.

In Ref. [18] – see also Refs. [19–23] –, concrete SUSY GUT models based on G_{PS} are constructed which naturally yield a moderate deviation from exact YU and, thus, can allow acceptable values of the b -quark mass for both signs of μ within the CMSSM. In particular, the Higgs sector of the simplest PS model [13, 14] is extended so that H_2 and H_1 are not exclusively contained in a $SU(4)_c$ singlet, $SU(2)_L \times SU(2)_R$ bidoublet superfield, but receive subdominant contributions from another bidoublet too which belongs to the adjoint rep-

*Electronic address: nikar@auth.gr

†Electronic address: lazaride@eng.auth.gr

‡Electronic address: kpallis@gen.auth.gr

representation of $SU(4)_c$. As a consequence, a modest violation of YU is naturally obtained, which can allow acceptable values of the b -quark mass even with universal boundary conditions. This approach is an alternative to the usual strategy [24–27] according to which YU is preserved, but the universal boundary conditions of the CMSSM are abandoned. We prefer to keep the universality hypothesis for the soft SUSY breaking rather than the exact Yukawa unification since we consider this hypothesis as more economical and predictive. Moreover, it can be easily accommodated within conventional SUSY GUT models. Indeed, it is known – cf. first paper in Ref. [26] – that possible violation of universality which could arise from D-term contributions if the MSSM is embedded into the PS GUT model does not occur provided that the soft SUSY breaking scalar masses of the super-heavy superfields which break the GUT gauge symmetry are assumed to be universal.

We will focus, as usually [18, 20, 21, 23], on the $\mu > 0$ case since $\mu < 0$ is strongly disfavored by the constraint arising from the deviation δa_μ of the measured value of the muon anomalous magnetic moment a_μ from its predicted value a_μ^{SM} in the SM. Indeed, $\mu < 0$ is defended [28] only at 3- σ by the calculation of a_μ^{SM} based on the τ -decay data, whereas there is a stronger and stronger tendency [29, 30] at present to prefer the e^+e^- -annihilation data for the calculation of a_μ^{SM} , which favor the $\mu > 0$ regime. Note that the results of Ref. [31], where it is claimed that the mismatch between the τ - and e^+e^- -based calculations is alleviated, disfavor $\mu < 0$ even more strongly.

The representation used for the Higgs superfield which mixes the $SU(2)_L$ doublets contained in the $SU(4)_c$ singlet and non-singlet Higgs bidoublets plays a crucial role in the proposal of Ref. [18]. As argued there, this Higgs superfield can be either a triplet or a singlet under $SU(2)_R$. In particular, it was shown that extending the PS model so as to include a pair of $SU(2)_R$ -triplet and/or a pair of $SU(2)_R$ -singlet Higgs superfields belonging to the adjoint representation of $SU(4)_c$ can lead to a sizable violation of YU. However, in the past, we mainly focused [18, 20, 21, 23] on the minimal extension of the PS model resulting from the inclusion of just a pair of $SU(2)_R$ -triplet superfields since this was enough to generate an adequate violation of YU ensuring, at the same time, a SUSY spectrum which leads to successful radiative electroweak symmetry breaking and a neutralino *lightest SUSY particle* (LSP) in a large fraction of the parametric space. The resulting asymptotic Yukawa quasi-unification conditions, which replaced the exact YU conditions, depend only on one new complex parameter (c) which was considered for simplicity real. It is also remarkable that this model predicts [21, 23] values for the mass m_h of the CP-even Higgs boson h close to those discovered [1–3] by the *Large Hadron Collider* (LHC) and supports new successful versions [32] of the F-term hybrid inflation based solely on renormalizable superpotential terms.

However, it has been recently recognized [23] that the lightest neutralino $\tilde{\chi}$ cannot act as a CDM candidate in this model. This is because the upper bound on the lightest neutralino relic density from CDM considerations, although this density is strongly reduced by neutralino-stau coannihilations, yields a very stringent upper bound on the mass of the lightest neutralino $m_{\tilde{\chi}}$, which is incompatible with the lower bound on $m_{\tilde{\chi}}$ from the data [33] on $\text{BR}(B_s \rightarrow \mu^+\mu^-)$. This result is further strengthened by the recent measurements [4] on $\text{BR}(B_s \rightarrow \mu^+\mu^-)$, which reduce the previous upper bound on this branching ratio and, thus, enhance even further the resulting lower bound on $m_{\tilde{\chi}}$. The main reason for this negative result is that $\tan\beta$ remains large and, thus, the SUSY contribution to $\text{BR}(B_s \rightarrow \mu^+\mu^-)$, which originates [34, 35] from neutral Higgs bosons in chargino-, H^\pm -, and W^\pm -mediated penguins and behaves as $\tan^6\beta/m_A^4$, turns out to be too large (m_A is the mass of CP-odd Higgs boson). Note, in passing, that even if one abandons universality in the electroweak Higgs sector and applies instead the boundary conditions of the so-called [22] NUHM1 model – with equal soft SUSY breaking masses for H_1 and H_2 , but different common soft mass m_0 for all the other scalar fields –, $\tan\beta$ still remains larger than about 55. Consequently, even in this case, compatibility of the data on $\text{BR}(B_s \rightarrow \mu^+\mu^-)$ [33] with the CDM bound on the neutralino relic density cannot be achieved – cf. Ref. [22].

Therefore, it would be interesting to check if, in the framework of the CMSSM and consistently with the GUT models of Ref. [18], we can revitalize the candidacy of $\tilde{\chi}$ as a CDM particle, circumventing the constraint from $\text{BR}(B_s \rightarrow \mu^+\mu^-)$ and, at the same time, obtaining experimentally acceptable m_h 's. A key-role in our present investigation is the inclusion of both pairs of $SU(2)_R$ -triplet and singlet Higgs superfields. This allows for a more general version of the Yukawa quasi-unification conditions – already extracted in Ref. [18] – which now depend on one real and two complex parameters. This liberates the third generation Yukawa coupling constants from the stringent constraint $h_b/h_t + h_\tau/h_t = 2$ obtained in the monoparametric case and, thus, can accommodate more general values of the ratios h_i/h_j with $i, j = t, b, \tau$, which are expected, of course, to be of order unity for natural values of the model parameters. This allows for lower $\tan\beta$'s and, consequently, the extracted $\text{BR}(B_s \rightarrow \mu^+\mu^-)$ can be reduced to an acceptable level compatible with the CDM requirement. The allowed parameter space of the model is then mainly determined by the interplay of the constraints from $\text{BR}(B_s \rightarrow \mu^+\mu^-)$ and CDM and the recently announced results of LHC on the Higgs mass m_h .

We first review the salient features of the PS GUT model in Sec. II and exhibit the cosmological and phenomenological requirements that we consider in our investigation in Sec. III. We then find the resulting restrictions on the parameter space of our model and test the perspective of direct neutralino detectability in Sec. IV. Finally, we summarize our conclusions in Sec. V.

II. VIOLATING YU WITHIN A SUSY PS MODEL

The starting point of our construction is the SUSY GUT model presented in Ref. [14]. It is based on G_{PS} , which, as already mentioned, is the simplest gauge group that can lead to YU. The representations and transformations under G_{PS} of the various matter and Higgs superfields of the model are presented in Table I ($U_c \in SU(4)_c$, $U_L \in SU(2)_L$, $U_R \in SU(2)_R$ and τ, \dagger , and $*$ stand for the transpose, the hermitian conjugate, and the complex conjugate of a matrix respectively). The model also possesses a Peccei-Quinn (PQ) symmetry, a $U(1)_R$ symmetry, and a discrete Z_2^{mp} matter parity symmetry with the charges of the superfields under these extra global symmetries also shown in Table I. The matter superfields are F_i and F_i^c ($i = 1, 2, 3$), while H_1 and H_2 belong to the superfield \mathcal{H} . So, as one can easily see, all the requirements [11] for exact YU are fulfilled. The breaking of G_{PS} down to the SM gauge group G_{SM} is achieved by the superheavy VEVs ($\sim M_{\text{GUT}}$) of the right handed neutrino type components ($\nu_H^c, \bar{\nu}_H^c$) of a conjugate pair of Higgs superfields H^c, \bar{H}^c . The model also contains a gauge singlet S which triggers the breaking of G_{PS} , a $SU(4)_c$ **6**-plet G which gives [13] masses to the right handed down quark type components of H^c, \bar{H}^c , and a pair of gauge singlets N, \bar{N} for solving [36] the μ problem of the MSSM via a PQ symmetry.

In order to allow for a sizable violation of YU, we extend the model by including three extra pairs of Higgs superfields $\mathcal{H}', \bar{\mathcal{H}}', \phi, \bar{\phi}$, and $\phi', \bar{\phi}'$, where the barred superfields are included in order to give superheavy masses to the unbarred superfields. These extra Higgs superfields together with their transformation properties and charges are also included in Table I. The superfield \mathcal{H}' belongs to the **(15, 2, 2)** representation of $SU(4)_c$ which is the only representation, besides **(1, 2, 2)**, that can couple to the fermions. On the other hand, ϕ and ϕ' acquire superheavy VEVs of order M_{GUT} after the breaking of G_{PS} to G_{SM} . Their couplings with $\bar{\mathcal{H}}'$ and \mathcal{H} naturally generate a $SU(2)_R$ - and $SU(4)_c$ -violating mixing of the $SU(2)_L$ doublets in \mathcal{H} and \mathcal{H}' leading, thereby, to a sizable violation of YU.

More explicitly, the part of the superpotential which is relevant for the breaking of G_{PS} to G_{SM} is given by

$$W_{\text{H}} = \kappa S (H^c \bar{H}^c - M^2) + m \phi \bar{\phi} + m' \phi' \bar{\phi}' - S (\beta \phi^2 + \beta' \phi'^2) + (\lambda \bar{\phi} + \lambda' \bar{\phi}') H^c \bar{H}^c, \quad (2)$$

where the mass parameters M, m , and m' are of order M_{GUT} , and $\kappa, \beta, \beta', \lambda$, and λ' are dimensionless parameters with $M, m, m', \kappa, \lambda, \lambda' > 0$ by field redefinitions. For simplicity, we take $\beta > 0$ and $\beta' > 0$ (the parameters are normalized so that they correspond to the couplings between the SM singlet components of the superfields).

TABLE I: Superfield Content of the Model

Super- fields	Representations	Transformations	Global Symmetries		
	under G_{PS}	under G_{PS}	R	PQ	Z_2^{mp}
Matter Fields					
F_i	$(\mathbf{4}, \mathbf{2}, \mathbf{1})$	$F_i U_L^\dagger U_c^\top$	$1/2$	-1	1
F_i^c	$(\bar{\mathbf{4}}, \mathbf{1}, \mathbf{2})$	$U_c^* U_R^* F_i^c$	$1/2$	0	-1
Higgs Fields					
H^c	$(\bar{\mathbf{4}}, \mathbf{1}, \mathbf{2})$	$U_c^* U_R^* H^c$	0	0	0
\bar{H}^c	$(\mathbf{4}, \mathbf{1}, \mathbf{2})$	$\bar{H}^c U_R^\top U_c^\top$	0	0	0
S	$(\mathbf{1}, \mathbf{1}, \mathbf{1})$	S	1	0	0
G	$(\mathbf{6}, \mathbf{1}, \mathbf{1})$	$U_c G U_c^\top$	1	0	0
\mathcal{H}	$(\mathbf{1}, \mathbf{2}, \mathbf{2})$	$U_L \mathcal{H} U_R^\top$	0	1	0
N	$(\mathbf{1}, \mathbf{1}, \mathbf{1})$	N	$1/2$	-1	0
\bar{N}	$(\mathbf{1}, \mathbf{1}, \mathbf{1})$	\bar{N}	0	1	0
Extra Higgs Fields					
\mathcal{H}'	$(\mathbf{15}, \mathbf{2}, \mathbf{2})$	$U_c^* U_L \mathcal{H}' U_R^\top U_c^\top$	0	1	0
$\bar{\mathcal{H}}'$	$(\mathbf{15}, \mathbf{2}, \mathbf{2})$	$U_c U_L \bar{\mathcal{H}}' U_R^\top U_c^\top$	1	-1	0
ϕ	$(\mathbf{15}, \mathbf{1}, \mathbf{3})$	$U_c U_R \phi U_R^\dagger U_c^\dagger$	0	0	0
$\bar{\phi}$	$(\mathbf{15}, \mathbf{1}, \mathbf{3})$	$U_c U_R \bar{\phi} U_R^\dagger U_c^\dagger$	1	0	0
ϕ'	$(\mathbf{15}, \mathbf{1}, \mathbf{1})$	$U_c \phi' U_c^\dagger$	0	0	0
$\bar{\phi}'$	$(\mathbf{15}, \mathbf{1}, \mathbf{1})$	$U_c \bar{\phi}' U_c^\dagger$	1	0	0

The scalar potential obtained from W_{H} is given by

$$V_{\text{H}} = |\kappa(H^c \bar{H}^c - M^2) - \beta \phi^2 - \beta' \phi'^2|^2 + |\kappa S + \lambda \bar{\phi} + \lambda' \bar{\phi}'|^2 (|H^c|^2 + |\bar{H}^c|^2) + |2\beta S \phi - m \bar{\phi}|^2 + |2\beta' S \phi' - m' \bar{\phi}'|^2 + |m \phi + \lambda H^c \bar{H}^c|^2 + |m' \phi' + \lambda' H^c \bar{H}^c|^2 + \text{D-terms}, \quad (3)$$

where the complex scalar fields which belong to the SM singlet components of the superfields are denoted by the same symbols as the corresponding superfields. Vanishing of the D-terms yields $\bar{H}^{c*} = e^{i\vartheta} H^c$ (H^c, \bar{H}^c lie in the $\nu_H^c, \bar{\nu}_H^c$ direction). We restrict ourselves to the direction with $\vartheta = 0$ which contains the SUSY vacua (see below). Performing appropriate R and gauge transformations, we bring H^c, \bar{H}^c and S to the positive real axis.

From the potential in Eq. (3), we find that the SUSY vacuum lies at

$$\langle H^c \bar{H}^c \rangle = v_0^2, \quad (4a)$$

$$\langle \phi \rangle = v_\phi \left(T_c^{15}, 1, \frac{\sigma_3}{\sqrt{2}} \right), \quad (4b)$$

$$\langle \phi' \rangle = v_{\phi'} \left(T_c^{15}, 1, \frac{\sigma_0}{\sqrt{2}} \right), \quad (4c)$$

and

$$\langle S \rangle = \langle \bar{\phi} \rangle = \langle \bar{\phi}' \rangle = 0, \quad (4d)$$

where

$$\left(\frac{v_0}{M}\right)^2 = \frac{1}{2\xi} \left(1 - \sqrt{1 - 4\xi}\right), \quad (4e)$$

$$v_\phi = -\lambda \frac{v_0^2}{m}, \quad v'_\phi = -\lambda' \frac{v_0^2}{m'} \quad (4f)$$

with

$$\xi = \frac{M^2}{\kappa} \left(\frac{\beta\lambda^2}{m^2} + \frac{\beta'\lambda'^2}{m'^2} \right) < 1/4. \quad (4g)$$

The structure of $\langle\phi\rangle$ and $\langle\phi'\rangle$ with respect to (w.r.t.) G_{PS} is shown in Eqs. (4b) and (4c), where

$$T_c^{15} = \frac{1}{2\sqrt{3}} \text{diag}(1, 1, 1, -3), \quad (5a)$$

$$\sigma_3 = \text{diag}(1, -1), \quad \text{and} \quad \sigma_0 = \text{diag}(1, 1). \quad (5b)$$

The part of the superpotential which is responsible for the mixing of the doublets in \mathcal{H} and \mathcal{H}' is

$$W_m = M_{\mathcal{H}} \bar{\mathcal{H}}' \mathcal{H}' + \lambda_3 \phi \bar{\mathcal{H}}' \mathcal{H} + \lambda_1 \phi' \bar{\mathcal{H}}' \mathcal{H}, \quad (6)$$

where the mass parameter $M_{\mathcal{H}}$ is of order M_{GUT} (made real and positive by field rephasing) and λ_3, λ_1 are dimensionless complex coupling constants. Note that the two last terms in the right hand side (RHS) of Eq. (6) overshadow the corresponding ones from the non-renormalizable $SU(2)_R$ -triplet and singlet couplings originating from the symbolic coupling $\bar{H}^c H^c \bar{\mathcal{H}}' \mathcal{H}$ (see Ref. [18]). Defining properly [18, 20] the relevant couplings in the RHS of Eq. (6), we obtain the mass terms

$$W_m = M_{\mathcal{H}} \bar{\mathcal{H}}_1^T \varepsilon (\mathcal{H}'_2 + \alpha_2 \mathcal{H}_2) + M_{\mathcal{H}} \left(\mathcal{H}_1^T + \alpha_1 \mathcal{H}_1^T \right) \varepsilon \bar{\mathcal{H}}'_2 + \dots, \quad (7)$$

where ε is the 2×2 antisymmetric matrix with $\varepsilon_{12} = 1$, the ellipsis includes color non-singlet components of the superfields, and the complex dimensionless parameters α_1 and α_2 are given by

$$\alpha_1 = \frac{1}{\sqrt{2}M_{\mathcal{H}}} (-\lambda_3 v_\phi + \lambda_1 v'_\phi), \quad (8a)$$

$$\alpha_2 = \frac{1}{\sqrt{2}M_{\mathcal{H}}} (\lambda_3 v_\phi + \lambda_1 v'_\phi). \quad (8b)$$

It is obvious from Eq. (7) that we obtain two pairs of superheavy doublets with mass $M_{\mathcal{H}}$:

$$\bar{\mathcal{H}}'_1, H'_2 \quad \text{and} \quad H'_1, \bar{\mathcal{H}}'_2, \quad (9a)$$

where

$$H'_r = \frac{\mathcal{H}'_r + \alpha_r \mathcal{H}_r}{\sqrt{1 + |\alpha_r|^2}}, \quad r = 1, 2 \quad (9b)$$

(no summation over the repeated index r is implied). The electroweak doublets H_r , which remain massless at the GUT scale, are orthogonal to the H'_r directions:

$$H_r = \frac{-\alpha_r^* \mathcal{H}'_r + \mathcal{H}_r}{\sqrt{1 + |\alpha_r|^2}}. \quad (10)$$

Solving Eqs. (9b) and (10) w.r.t. \mathcal{H}_r and \mathcal{H}'_r , we obtain

$$\mathcal{H}_r = \frac{H_r + \alpha_r^* \mathcal{H}'_r}{\sqrt{1 + |\alpha_r|^2}} \quad \text{and} \quad \mathcal{H}'_r = \frac{-\alpha_r H_r + \mathcal{H}'_r}{\sqrt{1 + |\alpha_r|^2}}. \quad (11)$$

The superheavy doublets H'_r must have zero VEVs, which gives

$$\langle \mathcal{H}_r \rangle = \frac{\langle H_r \rangle}{\sqrt{1 + |\alpha_r|^2}} \quad \text{and} \quad \langle \mathcal{H}'_r \rangle = \frac{-\alpha_r \langle H_r \rangle}{\sqrt{1 + |\alpha_r|^2}}. \quad (12)$$

The Yukawa interactions of the third family of fermions are described by the superpotential terms

$$W_Y = y_{33} F_3 \mathcal{H} F_3^c + 2y'_{33} F_3 \mathcal{H}' F_3^c, \quad (13)$$

where the factor of two is incorporated in the second term in the RHS of this equation in order to make y'_{33} directly comparable to y_{33} , since the doublets in \mathcal{H}' are proportional to T_c^{15} , which is normalized so that the trace of its square equals unity. From Eqs. (12) and (13) and using the fact that \mathcal{H}' is proportional to T_c^{15} in the $SU(4)_c$ space, we can readily derive the masses of the third generation fermions:

$$m_t = \left| \frac{1 - \rho \alpha_2 / \sqrt{3}}{(1 + |\alpha_2|^2)^{\frac{1}{2}}} y_{33} v_2 \right|, \quad (14a)$$

$$m_b = \left| \frac{1 - \rho \alpha_1 / \sqrt{3}}{(1 + |\alpha_1|^2)^{\frac{1}{2}}} y_{33} v_1 \right|, \quad (14b)$$

$$m_\tau = \left| \frac{1 + \sqrt{3} \rho \alpha_1}{(1 + |\alpha_1|^2)^{\frac{1}{2}}} y_{33} v_1 \right|, \quad (14c)$$

where $\rho \equiv y'_{33}/y_{33}$ can be made real and positive by readjusting the phases of \mathcal{H} , \mathcal{H}' and $v_r = \langle H_r \rangle$. The third generation Yukawa coupling constants (h_t, h_b , and h_τ) must then obey the following set of generalized asymptotic Yukawa quasi-unification conditions:

$$h_t(M_{\text{GUT}}) : h_b(M_{\text{GUT}}) : h_\tau(M_{\text{GUT}}) = \left| \frac{1 - \rho \alpha_2 / \sqrt{3}}{\sqrt{1 + |\alpha_2|^2}} \right| : \left| \frac{1 - \rho \alpha_1 / \sqrt{3}}{\sqrt{1 + |\alpha_1|^2}} \right| : \left| \frac{1 + \sqrt{3} \rho \alpha_1}{\sqrt{1 + |\alpha_1|^2}} \right|. \quad (15)$$

These conditions depend on two complex (α_1, α_2) and one real and positive (ρ) parameter. For natural values of ρ, α_1 , and α_2 , i.e. for values of these parameters which are of order unity and do not lead to unnaturally small numerators in the RHS of Eq. (15), we expect all the ratios h_i/h_j with $i, j = t, b, \tau$ to be of order unity. So, exact YU is naturally broken, but not completely lost since the ratios of the Yukawa coupling constants remain of order unity restricting, thereby, $\tan \beta$ to rather large values. On the other hand, these ratios do not have to obey any exact relation among themselves as in the previously studied [18–21, 23] monoparametric case. This gives us an extra freedom which allows us to satisfy all the phenomenological and cosmological requirements with the lightest neutralino contributing to CDM.

III. COSMOLOGICAL AND PHENOMENOLOGICAL CONSTRAINTS

The two-loop renormalization group equations for the Yukawa and the gauge coupling constants and the one-loop ones for the soft SUSY breaking parameters are used between the GUT scale M_{GUT} and a common SUSY threshold $M_{\text{SUSY}} \simeq (m_{\tilde{t}_1} m_{\tilde{t}_2})^{1/2}$ ($\tilde{t}_{1,2}$ are the stop mass eigenstates), which is determined consistently with the SUSY spectrum. At M_{SUSY} , we impose the conditions for radiative electroweak symmetry breaking, calculate the SUSY spectrum employing the publicly available code `SOFTSUSY` [37], and include the SUSY corrections to the b -quark and τ -lepton masses [16]. The corrections to m_τ (almost 4%) lead [18, 19] to a small decrease of $\tan\beta$. The running of the Yukawa and gauge coupling constants from M_{SUSY} to M_Z is continued using the SM renormalization group equations.

The pole mass of the top quark is fixed at its central value $M_t = 173$ GeV [38], which corresponds to the running mass $m_t(m_t) = 164.6$ GeV. We adopt also the central value [39] of the $\overline{\text{MS}}$ b -quark mass $m_b(m_b)^{\overline{\text{MS}}} = 4.19$ GeV, which is evolved up to M_Z using the central value $\alpha_s(M_Z) = 0.1184$ [39] of the strong fine structure constant and then converted [40] to the b -quark mass in the $\overline{\text{DR}}$ scheme at M_Z yielding $m_b(M_Z) = 2.84$ GeV. Finally, the tau-lepton mass is taken to be $m_\tau(M_Z) = 1.748$ GeV.

The model parameters are restricted by a number of phenomenological and cosmological constraints, which are evaluated by employing the latest version of the publicly available code `micrOMEGAs` [41]. We now briefly discuss these requirements paying special attention to those which are most relevant to our investigation.

a. Cold Dark Matter Considerations. The 95% c.l. range for the CDM abundance, according to the results of WMAP [5], is

$$\Omega_{\text{CDM}} h^2 = 0.1126 \pm 0.0072. \quad (16)$$

In the CMSSM, the LSP can be the lightest neutralino $\tilde{\chi}$ and naturally arises as a CDM candidate. The requirement that its relic abundance $\Omega_{\text{LSP}} h^2$ does not exceed the 95% c.l. upper bound derived from Eq. (16), i.e.

$$\Omega_{\text{LSP}} h^2 \lesssim 0.12, \quad (17)$$

strongly restricts the parameter space of the model, since $\Omega_{\text{LSP}} h^2$ generally increases with the mass of the LSP m_{LSP} and so an upper bound on m_{LSP} can be derived from Eq. (17). The lower bound on $\Omega_{\text{LSP}} h^2$ is not taken into account in our analysis since other production mechanisms [42] of LSPs may be present too and/or other particles [43, 44] may also contribute to the CDM. We calculate $\Omega_{\text{LSP}} h^2$ using the `micrOMEGAs` code, which includes accurately thermally averaged exact tree-level cross sections of all the (co)annihilation processes [9, 45], treats poles [10, 18, 46] properly, and uses one-loop QCD and SUSY QCD corrected [15, 18, 47] Higgs decay widths and couplings to fermions.

b. The Higgs Boson Mass. According to recent independent announcements from the ATLAS [1] and the CMS [2] experimental teams at the LHC – see also Ref. [3] – a discovered particle, whose behavior so far has been consistent with the SM-like Higgs boson, has mass around 125–126 GeV. More precisely the reported mass is $(126.0 \pm 0.4 \pm 0.4)$ GeV [1] or $(125.3 \pm 0.4 \pm 0.5)$ GeV [2]. In the absence of an official combination of these results and allowing for a theoretical uncertainty of ± 1.5 GeV, we construct a $2 - \sigma$ range adding in quadrature the various experimental and theoretical uncertainties and taking the upper [lower] bound from the ATLAS [CMS] results:

$$122 \lesssim m_h / \text{GeV} \lesssim 129.2. \quad (18)$$

This restriction is applied to the mass m_h of the CP-even Higgs boson h of MSSM. The calculation of m_h in the package `SOFTSUSY` [37] includes the full one-loop SUSY corrections and some zero-momentum two-loop corrections [48]. The results are well tested [49] against other spectrum calculators.

c. B-Physics Constraints. We also consider the following constraints originating from B -meson physics:

- The branching ratio $\text{BR}(B_s \rightarrow \mu^+ \mu^-)$ of the process $B_s \rightarrow \mu^+ \mu^-$ [34, 35] is to be consistent with the 95% c.l. bound [4]:

$$\text{BR}(B_s \rightarrow \mu^+ \mu^-) \lesssim 4.2 \times 10^{-9}, \quad (19)$$

which is significantly reduced relative to the previous experimental upper bound [33] adopted in Ref. [23]. This bound implies a lower bound on m_{LSP} since $\text{BR}(B_s \rightarrow \mu^+ \mu^-)$ decreases as m_{LSP} increases. Note that, very recently, the LHCb collaboration reported [50] a first evidence for the decay $B_s \rightarrow \mu^+ \mu^-$ yielding the following two sided 95% c.l. bound

$$1.1 \lesssim \text{BR}(B_s \rightarrow \mu^+ \mu^-) / 10^{-9} \lesssim 6.4. \quad (20)$$

In spite of this newer experimental upper bound on $\text{BR}(B_s \rightarrow \mu^+ \mu^-)$, we adopt here the much tighter upper bound on $\text{BR}(B_s \rightarrow \mu^+ \mu^-)$ in Eq. (19) since we consider it more realistic. As we show below, the upper bound on the LSP mass m_{LSP} which can be inferred from the lower bound on $\text{BR}(B_s \rightarrow \mu^+ \mu^-)$ in Eq. (20) does not constrain the parameters of our model.

- The branching ratio $\text{BR}(b \rightarrow s\gamma)$ of the process $b \rightarrow s\gamma$ [47, 51] is to be compatible with the 95% c.l. range [21, 52, 53]:

$$2.84 \times 10^{-4} \lesssim \text{BR}(b \rightarrow s\gamma) \lesssim 4.2 \times 10^{-4}. \quad (21)$$

Note that the SM plus the H^\pm and SUSY contributions [47, 51] to $\text{BR}(b \rightarrow s\gamma)$ initially increases with m_{LSP} and yields a lower bound on m_{LSP} from the lower bound in Eq. (21) – for higher values of m_{LSP} , it starts mildly decreasing.

- The ratio $R(B_u \rightarrow \tau\nu)$ of the CMSSM to the SM branching ratio of $B_u \rightarrow \tau\nu$ [35, 54] is to be confined in the 95% c.l. range [52] :

$$0.52 \lesssim R(B_u \rightarrow \tau\nu) \lesssim 2.04. \quad (22)$$

A lower bound on m_{LSP} can be derived from the lower bound in this inequality.

d. Muon Anomalous Magnetic Moment. The discrepancy δa_μ between the measured value a_μ of the muon anomalous magnetic moment and its predicted value in the SM can be attributed to SUSY contributions arising from chargino-sneutrino and neutralino-smuon loops. The relevant calculation is based on the formulas of Ref. [55]. The absolute value of the result decreases as m_{LSP} increases and its sign is positive for $\mu > 0$. On the other hand, the calculation of a_μ^{SM} is not yet stabilized mainly because of the ambiguities in the calculation of the hadronic vacuum-polarization contribution. According to the evaluation of this contribution in Ref. [28], there is still a discrepancy between the findings based on the e^+e^- -annihilation data and the ones based on the τ -decay data – however, in Ref. [31], it is claimed that this discrepancy can be alleviated. Taking into account the more reliable calculation based on the e^+e^- data [29], the recent complete tenth-order QED contribution [30], and the experimental measurements [56] of a_μ , we end up with a $2.9 - \sigma$ discrepancy

$$\delta a_\mu = (24.9 \pm 8.7) \times 10^{-10}, \quad (23)$$

resulting to the following 95% c.l. range:

$$7.5 \times 10^{-10} \lesssim \delta a_\mu \lesssim 42.3 \times 10^{-10}. \quad (24)$$

A lower [upper] bound on m_{LSP} can be derived from the upper [lower] bound in Eq. (24). As it turns out, only the upper bound on m_{LSP} is relevant here. Taking into account the aforementioned computational instabilities and the fact that a discrepancy at the level of about $3 - \sigma$ cannot firmly establish a real deviation from the SM value, we restrict ourselves to just mentioning at which level Eq. (23) is satisfied in the parameter space allowed by all the other constraints – cf. Ref. [6].

IV. RESTRICTIONS ON THE SUSY PARAMETERS

Imposing the requirements above, we can delineate the allowed parameter space. We find that the only constraints which play a role are the CDM bound in Eq. (17), the lower bound on m_h in Eq. (18), and the bound on $\text{BR}(B_s \rightarrow \mu^+\mu^-)$ in Eq. (19). In the parameter space allowed by these requirements, all the other restrictions of Sec. III are automatically satisfied with the exception of the lower bound on δa_μ in Eq. (24). This bound will not be imposed here as a strict constraint on the parameters of the model for the reasons explained in Sec. III.

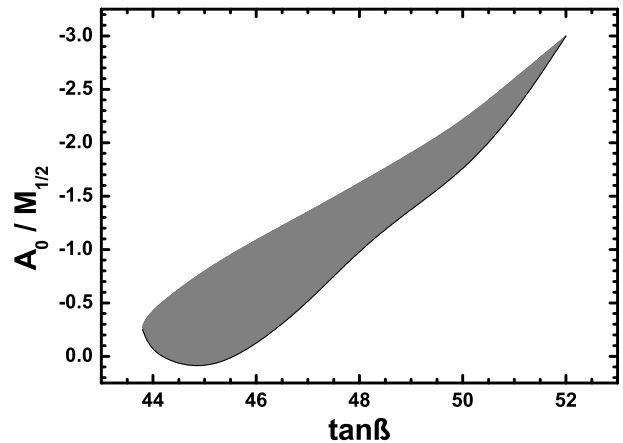


FIG. 1: The overall (shaded) allowed parameter space of the model in the $\tan\beta - A_0/M_{1/2}$ plane.

We will only discuss at which level Eq. (23) is satisfied in the parameter space allowed by the other requirements.

In Fig. 1, we present the overall allowed parameter space in the $\tan\beta - A_0/M_{1/2}$ plane. Each point in this shaded space corresponds to an allowed area in the $M_{1/2} - m_0$ plane (see below). The lower boundary of the allowed parameter space in Fig. 1 originates from the limit on $\text{BR}(B_s \rightarrow \mu^+\mu^-)$ in Eq. (19), except its leftmost part which comes from the lower bound on m_h in Eq. (18) or the CDM bound in Eq. (17). The upper boundary comes from the CDM bound in Eq. (17). We see that $\tan\beta$ ranges from about 43.8 to 52. These values are only a little smaller than the ones obtained for exact YU or the monoparametric Yukawa quasi-unification conditions discussed in Refs. [18, 20, 21, 23]. This mild reduction of $\tan\beta$ is, however, adequate to reduce the extracted $\text{BR}(B_s \rightarrow \mu^+\mu^-)$ to an acceptable level compatible with the CDM requirement. In the allowed area of Fig. 1, the parameter $A_0/M_{1/2}$ ranges from about -3 to 0.1 . We also find that, in this allowed area, the Higgs mass m_h ranges from 122 to 127.23 GeV and the LSP mass m_{LSP} from about 746.5 to 1433 GeV. So we see that, although m_h 's favored by LHC can be easily accommodated, the lightest neutralino mass is large making its direct detection very difficult. At the maximum allowed m_{LSP} , $\text{BR}(B_s \rightarrow \mu^+\mu^-)$ takes its minimal value in the allowed parameter space. This value turns out to be about 3.64×10^{-9} and, thus, the lower bound in Eq. (20) is satisfied everywhere in the allowed area in Fig. 1. The range of the discrepancy δa_μ between the measured muon anomalous magnetic moment and its SM value in the allowed parameter space of Fig. 1 is about $(0.35 - 2.76) \times 10^{-10}$ (note that δa_μ decreases as $\tan\beta$ or $M_{1/2}$ increases). Therefore, Eq. (23) is satisfied only at the level of 2.55 to $2.82 - \sigma$. Note that had we considered the $\mu < 0$ case, δa_μ would have been negative and the violation of Eq. (23) would have certainly been stronger than in the $\mu > 0$ case.

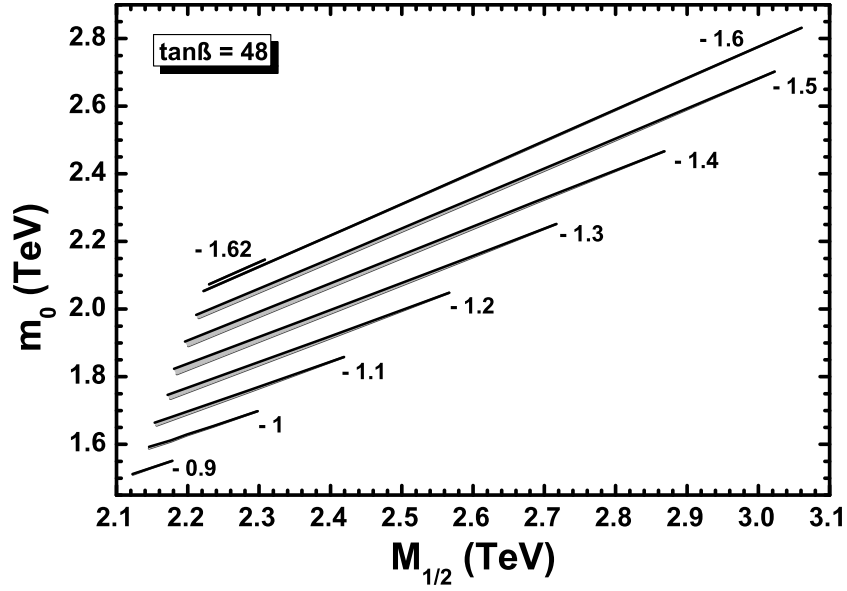


FIG. 2: The allowed (shaded) areas in the $M_{1/2} - m_0$ plane for $\tan\beta = 48$ and various $A_0/M_{1/2}$'s indicated on the graph.

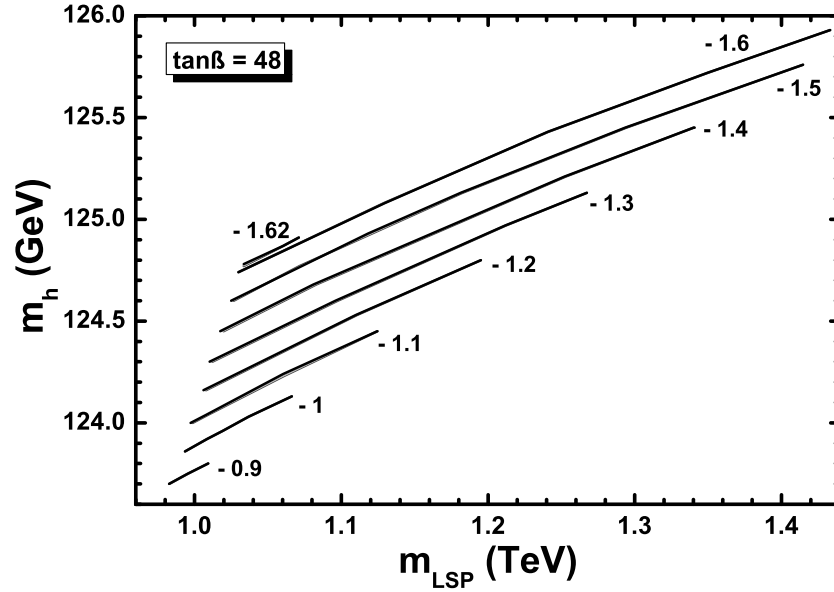


FIG. 3: The allowed (shaded) areas in the $m_{LSP} - m_h$ plane for $\tan\beta = 48$ and various $A_0/M_{1/2}$'s indicated on the graph.

In order to get a better understanding of the structure of the allowed parameter space and the role played by the various restrictions, we will now concentrate on the central value of $\tan\beta = 48$ and delineate the allowed areas in the $M_{1/2} - m_0$ and $m_{LSP} - m_h$ plane for various values of $A_0/M_{1/2}$. These allowed areas are the shaded areas in Figs. 2 and 3. We observe that these areas are very thin strips. Their lower boundary corresponds to $\Delta_{\tilde{\tau}_2} = 0$, where $\Delta_{\tilde{\tau}_2} = (m_{\tilde{\tau}_2} - m_{LSP})/m_{LSP}$ is the relative mass splitting between the lightest stau mass eigen-

state $\tilde{\tau}_2$, which is the next-to-LSP, and the LSP. The area below this boundary is excluded because the LSP is the charged $\tilde{\tau}_2$. The upper boundary of the areas comes from the CDM bound in Eq. (17), while the left one originates from the limit on $\text{BR}(B_s \rightarrow \mu^+ \mu^-)$ in Eq. (19). The upper right corner of the areas coincides with the intersection of the lines $\Delta_{\tilde{\tau}_2} = 0$ and $\Omega_{LSP} h^2 = 0.12$. We observe that the allowed area, starting from being just a point at $A_0/M_{1/2}$ slightly bigger than -0.9 , gradually expands as $A_0/M_{1/2}$ decreases and reaches its maximal size around

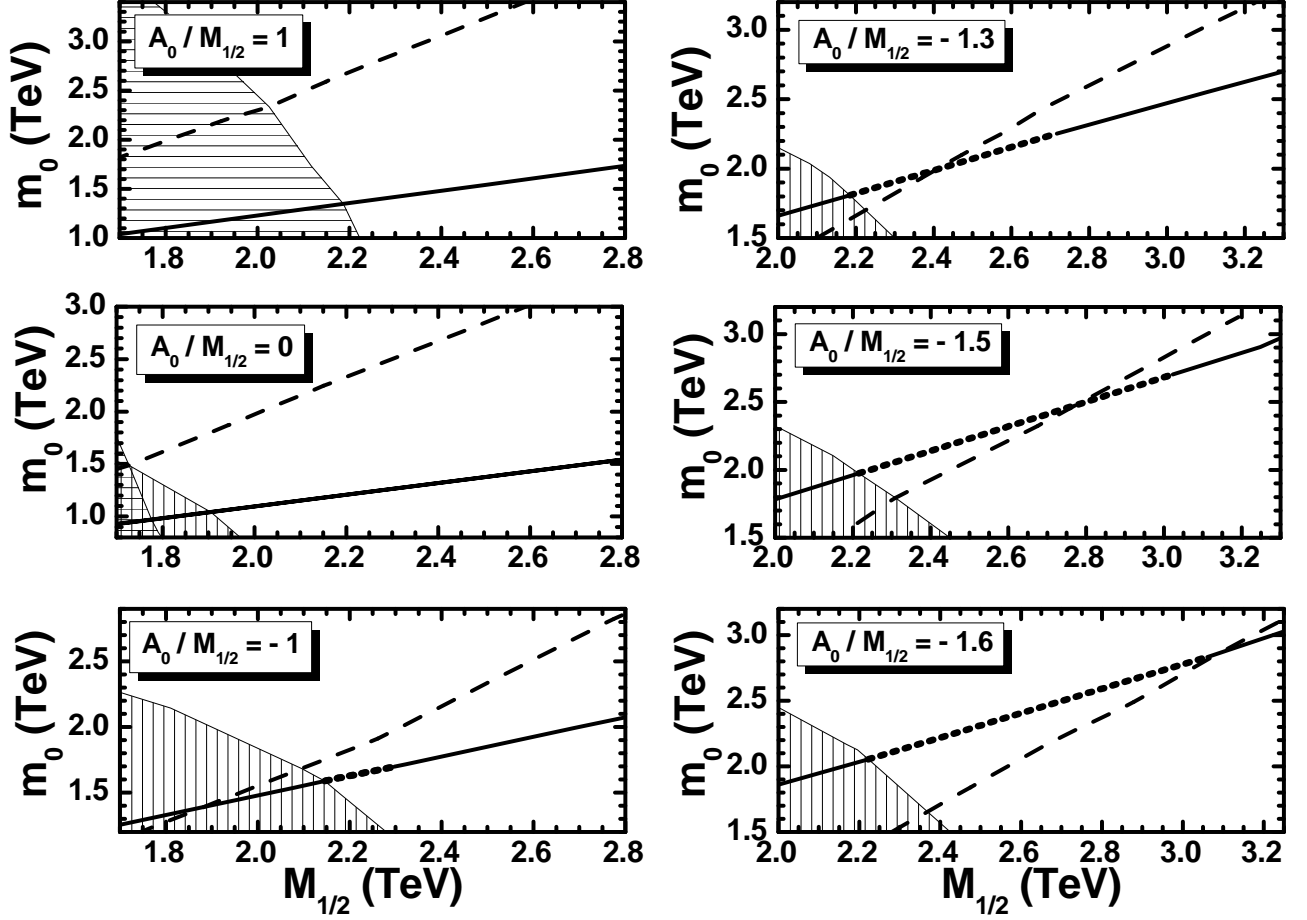


FIG. 4: Relative position of the $\Delta_{\tilde{\tau}_2} = 0$ (solid) line (with the dotted part included) and $\Delta_H = 0$ (dashed) line for $\tan \beta = 48$ and various $A_0/M_{1/2}$'s indicated on the graphs. Vertically [horizontally] hatched regions are excluded by the bound in Eq. (19) [lower bound in Eq. (18)]. The dotted areas are the overall allowed areas.

$A_0/M_{1/2} = -1.6$. For smaller $A_0/M_{1/2}$'s, it shrinks very quickly and disappears just after $A_0/M_{1/2} = -1.62$. We find that, for $\tan \beta = 48$, m_{LSP} ranges from about 983 to 1433 GeV, while m_h from about 123.7 to 125.93 GeV.

We will now discuss the structure of the allowed areas in Figs. 2 and 3. The fact that they are narrow strips along the lines with $\Delta_{\tilde{\tau}_2} = 0$ indicates that the main mechanism which reduces $\Omega_{\text{LSP}} h^2$ below 0.12 is the coannihilation of $\tilde{\tau}_2$'s and $\tilde{\chi}$'s. Indeed, we find that the dominant processes are the $\tilde{\tau}_2 \tilde{\tau}_2^*$ coannihilations to $b\bar{b}$ and $\tau\bar{\tau}$ contributing to the inverse of $\Omega_{\text{LSP}} h^2$ about (55 – 72)% and (11 – 15)% respectively. As already noticed in Ref. [6], these processes are enhanced by the s -channel exchange of the heavy CP-even neutral Higgs boson H , with mass m_H , in the presence of a resonance ($2m_{\text{LSP}} \simeq m_H$) – for the relevant channels, see, for example, Ref. [45]. In order to pinpoint the effect of the H -pole on the $\tilde{\tau}_2 \tilde{\tau}_2^*$ coannihilations, we must track its position relative to the line $\Delta_{\tilde{\tau}_2} = 0$. In Fig. 4, the dashed lines correspond to the H -pole, i.e. to $\Delta_H = 0$ with $\Delta_H = (m_H - 2m_{\text{LSP}})/2m_{\text{LSP}}$ for $\tan \beta = 48$ and various values of $A_0/M_{1/2}$ as indicated. The solid lines

(with their dotted part included) correspond to $\Delta_{\tilde{\tau}_2} = 0$ and the vertically [horizontally] hatched regions are excluded by the bound on $\text{BR}(B_s \rightarrow \mu^+ \mu^-)$ in Eq. (19) [lower bound on m_h in Eq. (18)]. We observe that, for $A_0/M_{1/2} = 1$, the lower bound on $M_{1/2}$ which originates from the lower bound on m_h in Eq. (18) overshadows the one from Eq. (19). In all other cases, however, we have the opposite situation. This is consistent with the fact that for almost fixed $M_{1/2}$ and m_0 , the Higgs mass m_h increases as $A_0/M_{1/2}$ decreases – cf. Ref. [6].

From Fig. 4, we see that, for $A_0/M_{1/2} = 1$ and 0, the H -pole line is far from the part of the $\Delta_{\tilde{\tau}_2} = 0$ line allowed by all the other constraints without considering the CDM bound. Consequently, in the neighborhood of this part, the effect of the H -pole is not strong enough to reduce $\Omega_{\text{LSP}} h^2$ below 0.12 via $\tilde{\tau}_2 \tilde{\tau}_2^*$ coannihilations and no overall allowed area exists. On the contrary, for $A_0/M_{1/2} = -1$, the H -pole line gets near the otherwise allowed (i.e. allowed by all the other requirements without considering the CDM bound) part of the $\Delta_{\tilde{\tau}_2} = 0$ line and starts affecting the neighborhood of its leftmost segment, where $\Omega_{\text{LSP}} h^2$ becomes smaller than

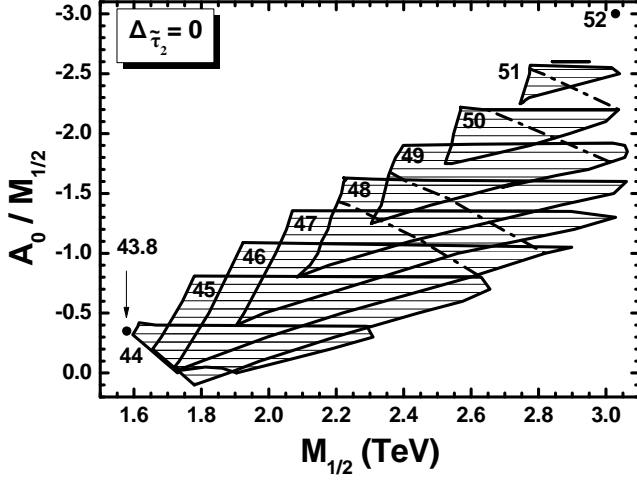


FIG. 5: Allowed regions in the $M_{1/2} - A_0/M_{1/2}$ plane for $\Delta\tilde{\tau}_2 = 0$ and various $\tan\beta$'s indicated on the graph. The dot-dashed lines from top to bottom correspond to $m_h = 126.5, 126, 125, 124.5$ GeV.

0.12 and, thus, an overall allowed (dotted) area appears. For $A_0/M_{1/2} = -1.3, -1.5, -1.6$, the H -pole line moves downwards and intersects the $\Delta\tilde{\tau}_2 = 0$ line with the point of intersection moving to the right as $A_0/M_{1/2}$ decreases. This enhances H -pole $\tilde{\tau}_2\tilde{\tau}_2^*$ coannihilation in the neighborhood of a bigger and bigger segment of the otherwise allowed part of the $\Delta\tilde{\tau}_2 = 0$ line and, thus, leads to $\Omega_{\text{LSP}}h^2$'s below 0.12 generating an overall allowed (dotted) area. For even smaller $A_0/M_{1/2}$'s, the H -pole line keeps moving downwards and gets away from most of the otherwise allowed part of the $\Delta\tilde{\tau}_2 = 0$ line. Also, the intersection of these two lines moves to higher values of $M_{1/2}$ and m_0 and the effect of the H -pole is weakened even around this intersection. So the overall allowed area quickly disappears as $A_0/M_{1/2}$ moves below -1.6 .

As we have seen, in the allowed parameter space of our model, $\Delta\tilde{\tau}_2$ is very close to zero. So we can restrict ourselves to $\Delta\tilde{\tau}_2 = 0$ without much loss. Note, by the way, that this choice ensures the maximal possible reduction of $\Omega_{\text{LSP}}h^2$ due to $\tilde{\tau}_2\tilde{\tau}_2^*$ coannihilations and, thus, leads to the maximal allowed $M_{1/2}$ [or m_{LSP}] for given $\tan\beta$, $A_0/M_{1/2}$, and m_0 [or m_h]. In Fig. 5, we present the allowed areas in the $M_{1/2} - A_0/M_{1/2}$ plane for $\Delta\tilde{\tau}_2 = 0$ and various values of $\tan\beta$ indicated on the graph. They are the horizontally hatched regions. Their right boundaries correspond to $\Omega_{\text{LSP}}h^2 = 0.12$, while the left ones saturate the bound on $\text{BR}(B_s \rightarrow \mu^+\mu^-)$ in Eq. (19) – cf. Fig. 1. The almost horizontal upper boundaries correspond to the sudden shrinking of the allowed areas which, as already discussed, is due to the weakening of the H -pole effect as $A_0/M_{1/2}$ drops below a certain value for each $\tan\beta$. The lower left boundary of the areas for $\tan\beta = 44, 45$, and 46 comes for the lower bound on m_h in Eq. (18), while the somewhat curved almost horizontal part of the lower boundary of the area for $\tan\beta = 44$ originates from the CDM bound in Eq. (17). The dot-dashed

TABLE II: Input and output parameters, masses of the sparticles and Higgses and values of the low energy observables of our model in four cases (recall that $1 \text{ pb} \simeq 2.6 \times 10^{-9} \text{ GeV}^{-2}$).

Input Parameters				
$\tan\beta$	48	49	50	51
$-A_0/M_{1/2}$	1.4	1.6	2	2.5
$M_{1/2}/\text{TeV}$	2.27	2.411	2.824	2.808
m_0/TeV	1.92	2.295	3.156	3.747
Output Parameters				
$h_t/h_\tau(M_{\text{GUT}})$	1.117	1.079	1.038	1.008
$h_b/h_\tau(M_{\text{GUT}})$	0.623	0.618	0.613	0.607
$h_t/h_b(M_{\text{GUT}})$	1.792	1.745	1.693	1.660
μ/TeV	2.78	3.092	3.823	4.129
$\Delta\tilde{\tau}_2(\%)$	1.43	0.93	0.1	0.17
$\Delta H(\%)$	3.08	1.30	0.11	1.76
Masses in TeV of Sparticles and Higgses				
$\tilde{\chi}$	1.023	1.110	1.309	1.303
$\tilde{\chi}_2^0$	1.952	2.117	2.489	2.481
$\tilde{\chi}_3^0$	2.782	3.088	3.815	4.114
$\tilde{\chi}_4^0$	2.785	3.091	3.817	4.116
$\tilde{\chi}_1^\pm$	1.985	2.117	2.489	2.481
$\tilde{\chi}_2^\pm$	2.785	3.091	3.817	4.116
\tilde{g}	4.809	5.190	6.042	6.040
\tilde{t}_1	3.806	4.097	4.761	4.781
\tilde{t}_2	3.226	3.458	3.967	3.902
\tilde{b}_1	3.838	4.141	4.853	4.947
\tilde{b}_2	3.763	4.058	4.733	4.757
\tilde{u}_L	4.687	5.138	6.186	6.483
\tilde{u}_R	4.485	4.923	5.946	6.257
\tilde{d}_L	4.687	5.138	6.187	6.483
\tilde{d}_R	4.459	4.896	5.914	6.227
$\tilde{\tau}_1$	2.082	2.347	2.979	3.293
$\tilde{\tau}_2$	1.037	1.121	1.310	1.305
$\tilde{\nu}_\tau$	2.075	2.342	2.975	3.289
\tilde{e}_L	2.453	2.819	3.690	4.201
\tilde{e}_R	2.112	2.476	3.339	3.901
$\tilde{\nu}_e$	2.451	2.818	3.689	4.200
h	0.1245	0.125	0.126	0.1265
H	2.109	2.249	2.621	2.652
H^\pm	2.111	2.251	2.623	2.654
A	2.110	2.25	2.622	2.652
Low Energy Observables				
$10^4 \text{BR}(b \rightarrow s\gamma)$	3.25	3.25	3.26	3.26
$10^9 \text{BR}(B_s \rightarrow \mu^+\mu^-)$	4.17	4.15	3.98	4.17
$R(B_u \rightarrow \tau\nu)$	0.975	0.977	0.982	0.982
$10^{10} \delta a_\mu$	1.11	0.89	0.57	0.49
$\Omega_{\text{LSP}}h^2$	0.11	0.11	0.11	0.11
$\sigma_{\tilde{\chi}p}^{\text{SI}}/10^{-12} \text{pb}$	6.17	4.55	2.44	1.75
$\sigma_{\tilde{\chi}p}^{\text{SD}}/10^{-9} \text{pb}$	1.69	1.08	0.43	0.28

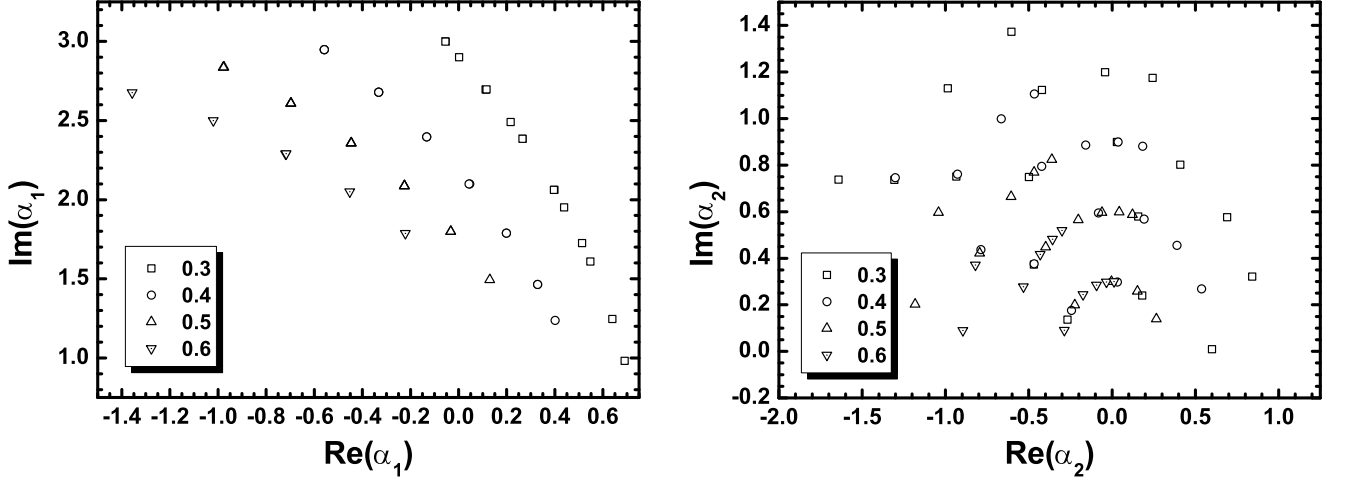


FIG. 6: The complex parameters α_1 and α_2 for various ρ 's indicated on the graphs for the case in the second column of Table II.

lines from top to bottom correspond to $m_h = 126.5, 126, 125, 124.5$ GeV. We see that the m_h 's which are favored by LHC can be readily obtained in our model for the higher allowed values of $\tan\beta$.

In Table II, we list the input and the output parameters of the present model, the masses in TeV of the SUSY particles – gauginos $\tilde{\chi}, \tilde{\chi}_2^0, \tilde{\chi}_3^0, \tilde{\chi}_4^0, \tilde{\chi}_1^\pm, \tilde{\chi}_2^\pm, \tilde{g}$, squarks $\tilde{t}_1, \tilde{t}_2, \tilde{b}_1, \tilde{b}_2, \tilde{u}_L, \tilde{u}_R, \tilde{d}_L, \tilde{d}_R$, and sleptons $\tilde{\tau}_1, \tilde{\tau}_2, \tilde{\nu}_\tau, \tilde{e}_L, \tilde{e}_R, \tilde{\nu}_e$ – and Higgses (h, H, H^\pm, A) and the values of the various low energy observables in four characteristic cases. Note that we consider the squarks and sleptons of the two first generations as degenerate. From the values of the various observable quantities it is easy to verify that all the relevant constraints are met. In the low energy observables, we included the spin-independent (SI) and spin-dependent (SD) lightest neutralino-proton ($\tilde{\chi} - p$) scattering cross sections $\sigma_{\tilde{\chi}p}^{\text{SI}}$ and $\sigma_{\tilde{\chi}p}^{\text{SD}}$, respectively, using central values for the hadronic inputs – for the details of the calculation, see Ref. [21]. We see that these cross sections are well below not only the present experimental upper bounds, but even the projected sensitivity of all planned future experiments. So the allowed parameter space of our model will not be accessible to the planned CDM direct detection experiments based on neutralino-proton scattering. We also notice that the sparticles turn out to be very heavy, which makes their discovery a very difficult task.

In the overall allowed parameter space of our model in Fig. 1, we find the following ranges for the ratios of the asymptotic third generation Yukawa coupling constants: $h_t/h_\tau \simeq 0.98 - 1.29$, $h_b/h_\tau \simeq 0.60 - 0.65$, and $h_t/h_b \simeq 1.62 - 2.00$. We observe that, although exact YU is broken, these ratios remain close to unity. They can generally be obtained by natural values of the real and positive parameter ρ and the complex parameters α_1, α_2 , which enter the Yukawa quasi-unification conditions in Eq. (15). Comparing these ratios with the ones

of the gauge coupling constants of the non-SUSY SM at a scale close to M_{GUT} – see e.g. Ref. [57] –, we can infer that the ratios here are not as close to unity. In spite of this, we apply the term Yukawa quasi-unification in the sense that the ratios of the Yukawa coupling constants in our model are much closer to unity than in generic models with lower values of $\tan\beta$ – cf. Ref. [58]. Finally, note that the deviation from exact YU here is comparable to the one obtained in the monparametric case – cf. Ref. [21] – and is also generated in a natural, systematic, controlled, and well-motivated manner.

In order to see this, we take as a characteristic example the second out of the four cases presented in Table II, which yields $m_h = 125$ GeV favored by the LHC. In this case, where $h_b/h_\tau = 0.618$ and $h_t/h_\tau = 1.079$, we solve Eq. (15) w.r.t. the complex parameters α_1, α_2 for various values of the real and positive parameter ρ . Needless to say that one can find infinitely many solutions since we have only two equations and five real unknowns. Some of these solutions are shown Fig. 6. Note that the equation for h_b/h_τ depends only on the combination $\rho\alpha_1$ and, thus, its solutions are expected to lie on a certain curve in the complex plane of this combination. Consequently, in the α_1 complex plane, the solutions should be distributed on a set of similar curves corresponding to the various values of ρ . This is indeed the case as one can see from the left panel of Fig. 6. For each α_1 and ρ in this panel, we then solve the equation for h_t/h_τ to find α_2 . In the right panel of Fig. 6, we show several such solutions. Observe that the equation for h_t/h_τ depends separately on α_2 and ρ and, thus, its solutions do not follow any specific pattern in the α_2 complex plane. Note that each point in the α_1 plane generally corresponds to more than one points in the α_2 plane. We scanned the range of ρ from 0.3 to 3 and found solutions only for the lower values of this parameter (up to about 0.6). The solutions found for α_1 and α_2 are also limited in certain natural re-

gions of the corresponding complex planes. The picture is very similar to the one just described for all the possible values of the ratios of the third generation Yukawa coupling constants encountered in our investigation. So we conclude that these ratios can be readily obtained by a multitude of natural choices of the parameters ρ , α_1 , and α_2 everywhere in the overall allowed parameter space of the model.

V. CONCLUSIONS

We performed an analysis of the parameter space of the CMSSM with $\mu > 0$ supplemented by a generalized asymptotic Yukawa coupling quasi-unification condition, which is implied by the SUSY GUT constructed in Ref. [18] and allows an experimentally acceptable b -quark mass. We imposed a number of cosmological and phenomenological constraints which originate from the CDM abundance in the universe, B physics ($b \rightarrow s\gamma$, $B_s \rightarrow \mu^+\mu^-$, and $B_u \rightarrow \tau\nu$), and the mass m_h of the lightest neutral CP-even Higgs boson. We found that, in contrast to previous results based on a more restrictive Yukawa quasi-unification condition, the lightest neutralino can act as a CDM candidate in a relatively wide range of parameters. In particular, the upper bound from CDM considerations on the lightest neutralino relic abundance, which is drastically reduced mainly by H -pole enhanced stau-antistau coannihilation processes, is

compatible with the recent data on the branching ratio of $B_s \rightarrow \mu^+\mu^-$ in this range of parameters. Also, values of $m_h \simeq (125-126)$ GeV, which are favored by LHC, can be easily accommodated. The mass of the lightest neutralino, though, comes out to be large (~ 1 TeV), which makes its direct detectability very difficult and the sparticle spectrum very heavy.

The fact that, in our model, $M_{1/2}$, m_0 , and μ generally turn out to be of the order of a few TeV puts under some stress the naturalness of the radiative electroweak symmetry breaking. This is, though, a general problem of the CMSSM especially in view of the recent data on the branching ratio of $B_s \rightarrow \mu^+\mu^-$ and the Higgs mass m_h as noted in Ref. [6, 58]. Indeed, these data not only strongly restrict the parameter space of the CMSSM so as to yield very heavy sparticle masses, but also make the electroweak symmetry breaking less natural.

Acknowledgments

We thank B.C. Allanach, A. Dedes, A.B. Lahanas, J. Rizos, V.C. Spanos, and N. Tetrakis for useful discussions. This work was supported by the European Union under the Marie Curie Initial Training Network ‘UNILHC’ PITN-GA-2009-237920 and the Greek Ministry of Education, Lifelong Learning and Religious Affairs and the Operational Program: Education and Lifelong Learning ‘HERACLITOS II’.

-
- [1] G. Aad *et al.* [ATLAS Collaboration], Phys. Lett. B **716**, 1 (2012).
 - [2] S. Chatrchyan *et al.* [CMS Collaboration], Phys. Lett. B **716**, 30 (2012).
 - [3] T. Aaltonen *et al.* [CDF and D0 Collaborations], Phys. Rev. Lett. **109**, 071804 (2012).
 - [4] R. Aaij *et al.* [LHCb Collaboration], Phys. Rev. Lett. **108**, 231801 (2012); J. Albrecht, Mod. Phys. Lett. A **27**, 1230028 (2012).
 - [5] E. Komatsu *et al.* [WMAP Collaboration], Astrophys. J. Suppl. **192**, 18 (2011); <http://lambda.gsfc.nasa.gov/product/map>.
 - [6] J. Cao, Z. Heng, D. Li, and J.M. Yang, Phys. Lett. B **710**, 665 (2012); J. Ellis and K.A. Olive, Eur. Phys. J. C **72**, 2005 (2012); H. Baer, V. Barger, P. Huang, and X. Tata, J. High Energy Phys. **05**, 109 (2012); A. Fowlie *et al.*, Phys. Rev. D **86**, 075010 (2012); O. Buchmueller *et al.*, arXiv:1207.7315;
 - [7] A.H. Chamseddine, R.L. Arnowitt, and P. Nath, Phys. Rev. Lett. **49**, 970 (1982); P. Nath, R.L. Arnowitt, and A.H. Chamseddine, Nucl. Phys. **B227**, 121 (1983); N. Ohta, Prog. Theor. Phys. **70**, 542 (1983); L.J. Hall, J.D. Lykken, and S. Weinberg, Phys. Rev. D **27**, 2359 (1983).
 - [8] R.L. Arnowitt and P. Nath, Phys. Rev. Lett. **69**, 725 (1992); G.G. Ross and R.G. Roberts, Nucl. Phys. **B377**, 571 (1992); V.D. Barger, M.S. Berger, and P. Ohmann, Phys. Rev. D **49**, 4908 (1994); G.L. Kane, C. Kolda, L. Roszkowski, and J.D. Wells, *ibid.* **49**, 6173 (1994).
 - [9] J.R. Ellis, T. Falk, and K.A. Olive, Phys. Lett. B **444**, 367 (1998); J.R. Ellis, T. Falk, K.A. Olive, and M. Srednicki, Astropart. Phys. **13**, 181 (2000); **15**, 413(E) (2001).
 - [10] A.B. Lahanas, D.V. Nanopoulos, and V.C. Spanos, Phys. Rev. D **62**, 023515 (2000); J.R. Ellis, T. Falk, G. Ganis, K.A. Olive, and M. Srednicki, Phys. Lett. B **510**, 236 (2001).
 - [11] G. Lazarides and C. Panagiotakopoulos, Phys. Lett. B **337**, 90 (1994); S. Khalil, G. Lazarides, and C. Pallis, *ibid.* **508**, 327 (2001).
 - [12] B. Ananthanarayan, G. Lazarides, and Q. Shafi, Phys. Rev. D **44**, 1613 (1991); Phys. Lett. B **300**, 245 (1993).
 - [13] I. Antoniadis and G.K. Leontaris, Phys. Lett. B **216**, 333 (1989).
 - [14] R. Jeannerot, S. Khalil, G. Lazarides, and Q. Shafi, J. High Energy Phys. **10**, 012 (2000).
 - [15] M.S. Carena, M. Olechowski, S. Pokorski, and C.E.M. Wagner, Nucl. Phys. **B426**, 269 (1994); R. Hempfling, Phys. Rev. D **49**, 6168 (1994); L.J. Hall, R. Rattazzi, and U. Sarid, *ibid.* **50**, 7048 (1994).
 - [16] D.M. Pierce, J.A. Bagger, K.T. Matchev, and R. Zhang, Nucl. Phys. **B491**, 3 (1997); M.S. Carena, D. Garcia, U. Nierste, and C.E.M. Wagner, *ibid.* **B577**, 88 (2000).
 - [17] P.Z. Skands *et al.*, J. High Energy Phys. **07**, 036 (2004).
 - [18] M.E. Gómez, G. Lazarides, and C. Pallis, Nucl. Phys. **B638**, 165 (2002).

- [19] M.E. Gómez, G. Lazarides, and C. Pallis, Phys. Rev. D **67**, 097701 (2003).
- [20] G. Lazarides and C. Pallis, hep-ph/0404266; hep-ph/0406081.
- [21] N. Karagiannakis, G. Lazarides, and C. Pallis, Phys. Lett. B **704**, 43 (2011).
- [22] S. Dar, I. Gogoladze, Q. Shafi, and C.S. Un, Phys. Rev. D **84**, 085015 (2011).
- [23] N. Karagiannakis, G. Lazarides, and C. Pallis, J. Phys. Conf. Ser. **384**, 012012 (2012); PoS CORFU **2011**, 023 (2011).
- [24] H. Baer, M.A. Diaz, J. Ferrandis, and X. Tata, Phys. Rev. D **61**, 111701 (2000); H. Baer, M. Brhlik, M.A. Diaz, J. Ferrandis, P. Mercadante, P. Quintana, and X. Tata, *ibid.* **63**, 015007 (2000); D. Auto, H. Baer, C. Balázs, A. Belyaev, J. Ferrandis, and X. Tata, J. High Energy Phys. **06**, 023 (2003); D. Auto, H. Baer, A. Belyaev, and T. Krupovnickas, *ibid.* **10**, 066 (2004).
- [25] T. Blažek, R. Dermíšek, and S. Raby, Phys. Rev. Lett. **88**, 111804 (2002); Phys. Rev. D **65**, 115004 (2002); R. Dermíšek, S. Raby, L. Roszkowski, and R. Ruiz de Austri, J. High Energy Phys. **04**, 037 (2003).
- [26] S.F. King and M. Oliveira, Phys. Rev. D **63**, 015010 (2001); I. Gogoladze, R. Khalid, and Q. Shafi, *ibid.* **79**, 115004 (2009); **80**, 095016 (2009); I. Gogoladze, R. Khalid, S. Raza, and Q. Shafi, arXiv:1008.2765.
- [27] U. Chattopadhyay and P. Nath, Phys. Rev. D **65**, 075009 (2002); U. Chattopadhyay, A. Corsetti, and P. Nath, *ibid.* **66**, 035003 (2002); C. Pallis, Nucl. Phys. **B678**, 398 (2004).
- [28] M. Davier, A. Hoecker, B. Malaescu, and Z. Zhang, Eur. Phys. J. C **71**, 1515 (2011); **72**, 1874(E) (2012).
- [29] K. Hagiwara, R. Liao, A.D. Martin, D. Nomura and T. Teubner, J. Phys. G **38**, 085003 (2011).
- [30] T. Aoyama, M. Hayakawa, T. Kinoshita, and M. Nio, Phys. Rev. Lett. **109**, 111808 (2012).
- [31] F. Jegerlehner and R. Szafron, Eur. Phys. J. C **71**, 1632 (2011); M. Benayoun, P. David, L. DelBuono, and F. Jegerlehner, *ibid.* **72**, 1848 (2012); arXiv:1210.7184.
- [32] R. Jeannerot, S. Khalil, and G. Lazarides, J. High Energy Phys. **07**, 069 (2002); G. Lazarides and A. Vamvasakis, Phys. Rev. D **76**, 083507 (2007); **76**, 123514 (2007); G. Lazarides, I.N.R. Peddie, and A. Vamvasakis, *ibid.* **78**, 043518 (2008); G. Lazarides, arXiv:1006.3636.
- [33] R. Aaij *et al.* [LHCb Collaboration], Phys. Lett. B **708**, 55 (2012).
- [34] P.H. Chankowski and L. Slawianowska, Phys. Rev. D **63**, 054012 (2001); C.S. Huang, W. Liao, Q.S. Yan, and S.H. Zhu, *ibid.* **63**, 114021 (2001); **64**, 059902(E) (2001); C. Bobeth, T. Ewerth, F. Kruger, and J. Urban, *ibid.* **64**, 074014 (2001); A. Dedes, H.K. Dreiner, and U. Nierste, Phys. Rev. Lett. **87**, 251804 (2001); J.R. Ellis, K.A. Olive, and V.C. Spanos, Phys. Lett. B **624**, 47 (2005).
- [35] F. Mahmoudi, Comput. Phys. Commun. **180**, 1579 (2009).
- [36] G. Lazarides and Q. Shafi, Phys. Rev. D **58**, 071702 (1998).
- [37] B.C. Allanach, Comput. Physics Commun. **143**, 305 (2002).
- [38] Tevatron Electroweak Working Group [CDF and D0 Collaborations], arXiv:0903.2503; T. Aaltonen *et al.* [CDF Collaboration], Phys. Rev. Lett. **105**, 252001 (2010).
- [39] K. Nakamura *et al.* [Particle Data Group], J. Phys. G **37**, 075021 (2010).
- [40] H. Baer, J. Ferrandis, K. Melnikov, and X. Tata, Phys. Rev. D **66**, 074007 (2002); K. Tobe and J.D. Wells, Nucl. Phys. **B663**, 123 (2003).
- [41] G. Belanger, F. Boudjema, A. Pukhov, and A. Semenov, <http://lapph.in2p3.fr/micromegas>; G. Belanger, F. Boudjema, P. Brun, A. Pukhov, S. Rosier-Lees, P. Salati, and A. Semenov, Comput. Phys. Commun. **182**, 842 (2011).
- [42] C. Pallis, Astropart. Phys. **21**, 689 (2004); J. Cosmol. Astropart. Phys. **10**, 015 (2005); Nucl. Phys. **B751**, 129 (2006); hep-ph/0610433.
- [43] L. Covi, L. Roszkowski, R. Ruiz de Austri, and M. Small, J. High Energy Phys. **06**, 003 (2004); K.-Y. Choi, L. Covi, J.E. Kim, and L. Roszkowski, *ibid.* **04**, 106 (2012).
- [44] H. Baer and H. Summy, Phys. Lett. B **666**, 5 (2008); H. Baer, M. Haider, S. Kraml, S. Sekmen, and H. Summy, J. Cosmol. Astropart. Phys. **02**, 002 (2009); H. Baer, A.D. Box, and H. Summy, J. High Energy Phys. **10**, 023 (2010).
- [45] M.E. Gómez, G. Lazarides, and C. Pallis, Phys. Rev. D **61**, 123512 (2000); Phys. Lett. B **487**, 313 (2000).
- [46] T. Nihei, L. Roszkowski, and R. Ruiz de Austri, J. High Energy Phys. **05**, 063 (2001); *ibid.* **07**, 024 (2002).
- [47] G. Bélanger, F. Boudjema, A. Pukhov, and A. Semenov, Comput. Phys. Commun. **174**, 577 (2006).
- [48] G. Degrossi, P. Slavich, and F. Zwirner, Nucl. Phys. **B611**, 403 (2001); A. Brignole, G. Degrossi, P. Slavich, and F. Zwirner, *ibid.* **B631**, 195 (2002); **B643**, 79 (2002); A. Dedes, G. Degrossi, and P. Slavich, *ibid.* **B672**, 144 (2003).
- [49] B.C. Allanach, S. Kraml, and W. Porod, J. High Energy Phys. **03**, 045 (2003); B.C. Allanach, A. Djouadi, J.L. Kneur, W. Porod, and P. Slavich, *ibid.* **09**, 044 (2004).
- [50] R. Aaij *et al.* [LHCb Collaboration], Phys. Rev. Lett. **110**, 021801 (2013).
- [51] M. Ciuchini, G. Degrossi, P. Gambino, and G.F. Giudice, Nucl. Phys. **B527**, 21 (1998); F. Borzumati and C. Greub, Phys. Rev. D **58**, 074004 (1998); G. Degrossi, P. Gambino, and G.F. Giudice, J. High Energy Phys. **12**, 009 (2000); M.E. Gómez, T. Ibrahim, P. Nath, and S. Skadhauge, Phys. Rev. D **74**, 015015 (2006).
- [52] E. Barberio *et al.* [Heavy Flavor Averaging Group], arXiv:0808.1297.
- [53] M. Misiak *et al.*, Phys. Rev. Lett. **98**, 022002 (2007).
- [54] G. Isidori and P. Paradisi, Phys. Lett. B **639**, 499 (2006); G. Isidori, F. Mescia, P. Paradisi, and D. Temes, Phys. Rev. D **75**, 115019 (2007).
- [55] S.P. Martin and J.D. Wells, Phys. Rev. D **64**, 035003 (2001).
- [56] G.W. Bennett *et al.* [Muon $g - 2$ Collaboration], Phys. Rev. D **73**, 072003 (2006).
- [57] H. Baer and X. Tata, *Weak Scale Supersymmetry: From Superfields to Scattering Events* (Cambridge University Press, Cambridge, UK, 2006).
- [58] S. Antusch, L. Calibbi, V. Maurer, M. Monaco, and M. Spinrath, Phys. Rev. D **85**, 035025 (2012); arXiv:1207.7236.